

A model of radiatively induced quark and lepton mass model

Takaaki Nomura

School of Physics, KIAS, Seoul 02455, Korea

E-mail: nomura@kias.re.kr

Abstract. We discuss a radiatively induced quark and lepton mass model in the first and second generation introducing extra $U(1)$ gauge symmetry, discrete Z_2 symmetry, vector-like fermions and exotic scalar fields. Then we analyze the allowed parameter regions which simultaneously satisfy the constraints of FCNCs for the quark sector and of LFVs including $\mu-e$ conversion, observed quark mass and mixing, and the lepton mass and mixing. In addition, the typical value for the $(g-2)_\mu$ in our model is presented. We also show extension of the model in which Majorana type neutrino masses are generated at the two loop level.

1. Introduction

The fermion masses in the standard model(SM) are hierarchical in both quark and lepton sector. In particular, masses of the SM neutrinos are very small compared to the other fermion masses. It is thus challenging to understand the hierarchical structure of fermion masses.

Radiative mass generation models are one of the interesting scenario to explain such a mass hierarchy in which some fermion masses are generated at loop levels and loop suppression factor would be a source of large mass difference. In addition, these models would lead rich phenomenology such as lepton flavor violation(LFV), anomalous muon magnetic dipole moment(muon $g-2$), flavor changing neutral current(FCNC) and existence of dark matter(DM) candidate.

In this proceeding, we review two radiative mass generation models where the second one is an extension of the first one [1, 2]. In our models, the first and second generation SM charged-lepton and quark masses are induced at one-loop level while the masses of third generation fermions are generated via the vacuum expectation value(VEV) of SM Higgs field. To realize our scenario, we add extra local $U(1)$ symmetry to restrict the Yukawa interaction associated with SM Higgs field in anomaly free way, and the vector-like quarks and leptons are introduced to write relevant one-loop diagrams for fermion mass generation. Therefore, the charged-lepton and quark masses in first two generations are generated at the one-loop level induced by the Yukawa interactions among SM fermions, inert scalar fields and vector-like fermions which are invariant under the new $U(1)$. The SM neutrino masses are generated at one-loop level as the other fermion masses in the first model while the second model realize two-loop level mass generation of neutrino [2]. Thus the smallness of the neutrino masses are naturally obtained in the second model. For both models, we search for the parameter range which can fit the observed fermion masses and mixing, taking into account the constraints from flavor physics. Note also that our model includes DM candidate whose relic density can be accommodated with



Table 1. Fermion contents in the model I with their charge assignments under $SU(2)_L \times U(1)_Y \times U(1)_R \times Z_2$, where each of the flavor index is defined as $\alpha \equiv 1 - 3$ and $i = 1, 2$.

Fermions	Q_L^α	u_R^i	d_R^i	t_R	b_R	$Q_{L(R)}^i$	L_L^α	e_R^i	ν_R^i	τ_R	$L_{L(R)}^i$
$SU(3)_C$	3	3	3	3	3	3	1	1	1	1	1
$SU(2)_L$	2	1	1	1	1	2	2	1	1	1	2
$U(1)_Y$	$\frac{1}{6}$	$\frac{2}{3}$	$-\frac{1}{3}$	$\frac{2}{3}$	$-\frac{1}{3}$	$\frac{1}{6}$	$-\frac{1}{2}$	-1	0	-1	$-\frac{1}{2}$
$U(1)_R$	0	x	$-x$	0	0	0	0	$-x$	x	0	0
Z_2	+	+	+	+	+	-	+	+	+	+	-

Table 2. Charge assignment for scalar fields in the model I.

Scalar fields	Φ	φ	η	S
$SU(2)_L$	2	1	2	1
$U(1)_Y$	$\frac{1}{2}$	0	$\frac{1}{2}$	0
$U(1)_R$	0	x	x	0
Z_2	+	+	-	-

observed value where we omit the discussion in order to focus on fermion mass sector; detailed discussions can be found in Ref. [2].

2. Model I

In this section, we introduce a model which is based on $G_{SM} \times U(1)_R \times Z_2$ symmetry; G_{SM} is the SM gauge symmetry and $U(1)_R$ is extra $U(1)$ gauge symmetry. Then we discuss fermion mass matrices, FCNC in quark sector and LFVs [1]. In our analysis, we assume Z' associated with $U(1)_R$ is sufficiently heavy avoiding experimental constraints and discussion of it is omitted.

2.1. Particle contents

The fermion contents are summarized in Table 1 where we introduce $SU(2)_L$ doublet exotic vector-like quarks $Q' \equiv [u', d']^T$ and leptons $L' \equiv [N', E']^T$ with two flavors. In addition we introduce two right-handed neutrinos ν_R^i ($i = 1, 2$), which constitute Dirac fields after the spontaneous electroweak symmetry breaking as the other fermion sectors in the SM. Then a gauged $U(1)_R$ symmetry is imposed where only the first and second family of right-handed SM fermions and ν_R^i have non-zero charge x ; the $U(1)_R$ is anomaly free by the charge assignment. Notice here that we require the third generation couple to the SM-like Higgs directly and masses of third generation fermions are generated at tree level.

The contents of scalar fields are summarized in Table 2 where we add two $SU(2)_L$ singlets φ and S , and one $SU(2)_L$ doublet scalar η to the SM Higgs-like field Φ ; here Φ and φ have the VEVs, symbolized by $\langle \Phi \rangle \equiv v/\sqrt{2}$ and $\langle \varphi \rangle \equiv v'/\sqrt{2}$, that spontaneously break the electroweak and $U(1)_R$ symmetry respectively, while S and η do not have VEVs that are assured by the Z_2 symmetry. Note also that S is assumed to be real scalar field.

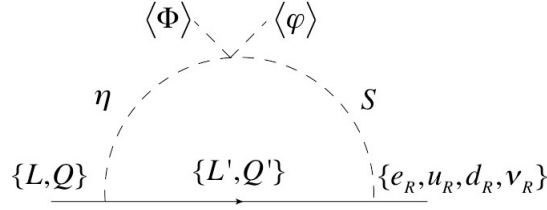


Figure 1. The one loop diagram for generating fermion masses.

Under symmetries in the model, the vector-like fermion mass term and Yukawa interactions are given by

$$-\mathcal{L}_Q = (y_u)_{ij} \bar{Q}'_i u_{Rj} (i\sigma_2) \eta^* + (y_d)_{ij} \bar{Q}'_i \eta d_{Rj} + (y_Q)_{\alpha j} \bar{Q}_\alpha Q'_j S + (y_t)_\alpha \bar{Q}_\alpha t_{Rj} (i\sigma_2) \Phi^* + (y_b)_\alpha \bar{Q}_\alpha \Phi b_R + m_{Q'_k} \bar{Q}'_k Q'_k + \text{c.c.}, \quad (1)$$

$$-\mathcal{L}_L = (y_\nu)_{ij} \bar{L}'_i \nu_{Rj} (i\sigma_2) \eta^* + (y_\ell)_{ij} \bar{L}'_i \eta e_{Rj} + (y_L)_{\alpha j} \bar{L}_\alpha L'_j S + (y_\tau)_\alpha \bar{L}_\alpha \tau_{Rj} (i\sigma_2) \Phi + (y_{\nu\tau})_\alpha \bar{L}_\alpha \Phi \nu_{\tau R} + m_{L'_k} \bar{L}'_k L'_k + \text{c.c.}, \quad (2)$$

where σ_2 is the second Pauli matrix.

The scalar potential in the model is given by

$$V = m_\varphi^2 |\varphi|^2 + m_S^2 S^2 + m_\Phi^2 |\Phi|^2 + m_\eta^2 |\eta|^2 + \lambda_0 \left[(\Phi^\dagger \eta) S \varphi^* + \text{c.c.} \right] \quad (3)$$

$$+ \lambda_\varphi |\varphi|^4 + \lambda_S S^4 + \lambda_\Phi |\Phi|^4 + \lambda_\eta |\eta|^4 + \lambda_{\varphi S} |\varphi|^2 S^2 + \lambda_{\varphi \Phi} |\varphi|^2 |\Phi|^2 + \lambda_{\varphi \eta} |\varphi|^2 |\eta|^2 + \lambda_{S\Phi} S^2 |\Phi|^2 + \lambda_{S\eta} S^2 |\eta|^2 + \lambda_{\Phi\eta} |\Phi|^2 |\eta|^2 + \lambda'_{\Phi\eta} |\Phi^\dagger \eta|^2. \quad (4)$$

We write scalar fields by components as

$$\Phi = \begin{bmatrix} w^+ \\ \frac{v+\phi+iz}{\sqrt{2}} \end{bmatrix}, \quad \eta = \begin{bmatrix} \eta^+ \\ \frac{\eta_R+i\eta_L}{\sqrt{2}} \end{bmatrix}, \quad \varphi = \frac{v' + \varphi_R + i\varphi_I}{\sqrt{2}}, \quad (5)$$

where w^\pm , z , and φ_I are Nambu-Goldstone(NG) bosons absorbed by the longitudinal degrees of freedom of charged SM gauged boson W^\pm , neutral SM gauge boson Z , and neutral $U(1)_R$ gauge boson Z' . After the spontaneous symmetry breaking, neutral scalar bosons mix each other as follows:

$$\begin{bmatrix} S \\ \eta_R \end{bmatrix} = \mathcal{O}_R \begin{bmatrix} H_1 \\ H_2 \end{bmatrix}, \quad \begin{bmatrix} \varphi_R \\ \phi \end{bmatrix} = \mathcal{O}_\beta \begin{bmatrix} h_1 \\ h_2 \end{bmatrix}, \quad \mathcal{O}_a \equiv \begin{bmatrix} c_a & s_a \\ -s_a & c_a \end{bmatrix}, \quad (6)$$

where $c_a \equiv \cos a$, $s_a \equiv \sin a$, $H_i (i = 1, 2)$ is the mass eigenstate of the inert neutral scalar boson, and $h_i (i = 1, 2)$ is the mass eigenstate of the Z_2 even neutral scalar boson.

By these interactions, first and second generation fermions masses are generated at one loop level as shown in Fig. 1. We discuss formula for the mass matrices below.

2.2. Quark sector

In this subsection, we analyze the quark sector including mass matrices and FCNC. The mass matrix in our form is written in terms of tree level mass matrix and one-loop one as

$$(M_{u(d)})_{\alpha\beta} = (M_{u(d)}^{tree})_{\alpha\beta} + (M_{u(d)}^{one-loop})_{\alpha\beta}, \quad (7)$$

with

$$(M_{u(d)}^{tree})_{\alpha 3} = \frac{(y_{t(b)})_{\alpha}}{\sqrt{2}}, \quad (8)$$

$$(M_{u(d)}^{one-loop})_{\alpha j} = s_R c_R \sum_{k=1,2} \frac{(y_Q)_{\alpha k} m_{Q'_k} (y_{u(d)})_{kj}}{\sqrt{2}(4\pi)^2} \int_0^1 dx_1 \frac{x_1 m_{Q'_k}^2 + (1-x_1)m_{H_1}^2}{x_1 m_{Q'_k}^2 + (1-x_1)m_{H_2}^2}. \quad (9)$$

As in the SM, up- and down-type quark mass matrices are diagonalized by $M_u^{diag.} = V_{uL} M_u V_{uR}$, and $M_d^{diag.} = V_{dL} M_d V_{dR}$, where V 's are unitary matrix. Then CKM matrix is defined by $V_{CKM} \equiv V_{uL}^\dagger V_{dL}$ which can be parametrized by three mixing angles and one phase as follows:

$$V_{CKM} \equiv V_{uL}^\dagger V_{dL} \equiv \begin{bmatrix} 1 & 0 & 0 \\ 0 & c_{23} & s_{23} \\ 0 & -s_{23} & c_{23} \end{bmatrix} \begin{bmatrix} c_{13} & 0 & s_{13}e^{-i\delta} \\ 0 & 1 & 0 \\ -s_{13}e^{i\delta} & 0 & c_{13} \end{bmatrix} \begin{bmatrix} c_{12} & s_{12}e^{-i\delta} & 0 \\ -s_{12} & c_{12} & 0 \\ 0 & 0 & 1 \end{bmatrix}. \quad (10)$$

In our numerical analysis, we assume to take the following forms to evade the stringent constraint of $B_0 - \bar{B}_0$ mixing in the numerical analysis:

$$V_{uL}^\dagger = \begin{bmatrix} 1 & 0 & 0 \\ 0 & c_{23} & s_{23} \\ 0 & -s_{23} & c_{23} \end{bmatrix} \begin{bmatrix} c_{13} & 0 & s_{13}e^{-i\delta} \\ 0 & 1 & 0 \\ -s_{13}e^{i\delta} & 0 & c_{13} \end{bmatrix}, \quad V_{dL} = \begin{bmatrix} c_{12} & s_{12}e^{-i\delta} & 0 \\ -s_{12} & c_{12} & 0 \\ 0 & 0 & 1 \end{bmatrix}. \quad (11)$$

The stringent constraints come from FCNCs where we consider $Q - \bar{Q}$ mixing inducing the mass difference between a meson and an anti-meson. Here we symbolize these observables by Δm_M where $M = D, K, B$ indicates the type of mesons. Then our formulas are given by calculating box-type one-loop diagrams by [3]

$$\Delta m_M \approx \frac{1}{2(4\pi)^2} \sum_{\rho, \sigma}^{1,2} (\mathcal{F}_{\rho\sigma}^- C_{Q_2}^M (\mathcal{M}_{Q_2}^M)^2_{\rho\sigma} + \mathcal{F}_{\rho\sigma}^+ C_{Q_4}^M (\mathcal{M}_{Q_4}^M)^2_{\rho\sigma}), \quad (12)$$

with

$$(\mathcal{M}_{Q_{2[4]}}^D)_{\rho\sigma}^2 \equiv (y'_u)_{\rho 2} m_{Q'_\rho} (y'_Q)_{1\rho} (y'_{Q[u]})_{1\sigma}^{\dagger} m_{Q'_\sigma} (y'_{u[Q]})_{\sigma 2}^{\dagger}, \quad (13)$$

$$(\mathcal{M}_{Q_{2[4]}}^K)_{\rho\sigma}^2 \equiv (y'_d)_{\rho 2} m_{Q'_\rho} (y'_Q)_{1\rho} (y'_{Q[d]})_{1\sigma}^{\dagger} m_{Q'_\sigma} (y'_{d[Q]})_{\sigma 2}^{\dagger}, \quad (14)$$

$$(\mathcal{M}_{Q_{2[4]}}^B)_{\rho\sigma}^2 \equiv (y'_d)_{\rho 3} m_{Q'_\rho} (y'_Q)_{1\rho} (y'_{Q[d]})_{1\sigma}^{\dagger} m_{Q'_\sigma} (y'_{d[Q]})_{\sigma 3}^{\dagger}, \quad (15)$$

$$C_{Q_2}^M = -\frac{5}{24} \left(\frac{m_M}{m_c + m_u} \right)^2 m_M f_M^2, \quad C_{Q_4}^M = \left[\frac{1}{24} + \frac{1}{4} \left(\frac{m_M}{m_c + m_u} \right)^2 \right] m_M f_M^2, \quad (16)$$

and

$$\mathcal{F}_{\rho\sigma}^\pm \equiv \left[\frac{s_{2R}^2}{2} (F_1[H_1] + F_1[H_2]) + c_{2R}^2 (F_2[H_1, H_2] + F_1[H_2, H_1]) \pm c_R^2 F_2[\eta_I, H_1] \pm s_R^2 F_2[\eta_I, H_2] \right]_{\rho\sigma}, \quad (17)$$

$$F_1[m_a] \equiv \int_0^1 da \int_0^{1-a} db \frac{1-a-c}{[am_{Q'_\rho}^2 + bm_{Q'_\sigma}^2 + (1-a-b)m_a^2]^2}, \quad (18)$$

$$F_2[m_a, m_b] \equiv \int_0^1 da \int_0^{1-a} db \int_0^{1-a-b} dc \frac{1}{[am_{Q'_\rho}^2 + bm_{Q'_\sigma}^2 + cm_a^2 + (1-a-b-c)m_b^2]^2}, \quad (19)$$

Table 3. Summary of constraints from LFV processes $\ell_j \rightarrow \ell_\alpha \gamma$ and $\mu \rightarrow e$ conversion.

Process	(j, α)	Experimental bounds (90% CL)	References
$\mu^- \rightarrow e^- \gamma$	(2, 1)	$BR(\mu \rightarrow e \gamma) < 4.2 \times 10^{-13}$	[5]
$\tau^- \rightarrow e^- \gamma$	(3, 1)	$Br(\tau \rightarrow e \gamma) < 3.3 \times 10^{-8}$	[6]
$\tau^- \rightarrow \mu^- \gamma$	(3, 2)	$BR(\tau \rightarrow \mu \gamma) < 4.4 \times 10^{-8}$	[6]
$\mu \rightarrow e$ conversion	(2, 1)	$R(Ti) < 4.3 \times 10^{-12} \rightarrow \mathcal{O}(10^{-18})$ (future bound)	[7] → [8]

where the Yukawa couplings are defined to be $y'_{u(d)} \equiv y_{u(d)} V_{u(d)R}^\dagger$, $y'_Q \equiv V_{uL} y_Q$, and we assume $V_L = V_R$ in our analytical convenience. Here experimental and input values [4] are given as follows:

$$m_u \approx 2.3[\text{MeV}], \quad m_c \approx 1275[\text{MeV}], \quad m_t \approx 173.2[\text{GeV}], \quad (20)$$

$$m_d \approx 4.8[\text{MeV}], \quad m_s \approx 95[\text{MeV}], \quad m_b \approx 4.18[\text{GeV}], \quad (21)$$

$$m_D \approx 1864.84[\text{MeV}], \quad m_K \approx 497.614[\text{MeV}], \quad m_B \approx 5279.50[\text{MeV}], \quad (22)$$

$$f_D \approx 212[\text{MeV}], \quad f_K \approx 159.8[\text{MeV}], \quad f_B \approx 200[\text{MeV}]. \quad (23)$$

Then we apply phenomenological bounds requiring that new physics contribution to Δm_M should be less than observed values [4]

$$\Delta m_D \lesssim 6.25 \times 10^{-12}[\text{MeV}], \quad \Delta m_K \lesssim 3.484 \times 10^{-12}[\text{MeV}], \quad \Delta m_B \lesssim 3.356 \times 10^{-10}[\text{MeV}]. \quad (24)$$

2.3. Lepton sector

In this subsection, we discuss the lepton sector including mass matrix and LFVs, where neutrinos are supposed to be Dirac neutrino. As in the quark sector, mass matrices can be given by

$$(M_{\nu(\ell)})_{\alpha\beta} = (M_\ell^{\text{tree}})_{\alpha\beta} + (M_{\nu(\ell)}^{\text{one-loop}})_{\alpha\beta}, \quad (25)$$

with

$$(M_\ell^{\text{tree}})_{\alpha\beta} = \frac{(y_\ell)_{\alpha\beta}}{\sqrt{2}}, \quad (26)$$

$$(M_{\nu(\ell)}^{\text{one-loop}})_{\alpha\beta} = s_R c_R \sum_{k=1,2} \frac{(y_{\nu(L)})_{\alpha k} m_{L'_k} (y_S)_{kj}}{\sqrt{2}(4\pi)^2} \int_0^1 dx_2 \frac{x_2 m_{L'_k}^2 + (1-x_2)m_{H_1}^2}{x_2 m_{L'_k}^2 + (1-x_2)m_{H_2}^2}. \quad (27)$$

The LFV processes give the constraints on our parameters. We firstly consider $\ell_j \rightarrow \ell_\alpha \gamma$ process, and its branching ratio is given by

$$BR(\ell_j \rightarrow \ell_\alpha \gamma) \approx \frac{48\pi^3 \alpha_{em} C_j}{G_F^2 m_{\ell_j}^2} |a_{j\alpha}|^2 \quad (28)$$

where $C_j = (1, 1/5)$ for $(i = \mu, \tau)$, $\alpha_{em} \approx 1/137$ is the fine-structure constant, $G_F \approx 1.17 \times 10^{-5} \text{ GeV}^{-2}$ is the Fermi constant, $a_{j\alpha}$ is computed as

$$a_{j\alpha} = -\frac{s_R c_R}{2\sqrt{2}(4\pi)^2} \sum_{k=1}^2 (y'_\ell)_{\alpha k} m_{L'_k} (y_{L'})_{kj} \left[F_{\ell_j \rightarrow \ell_\alpha \gamma}(m_{H_1}, m_{L'_k}) - F_{\ell_j \rightarrow \ell_\alpha \gamma}(m_{H_2}, m_{L'_k}) \right], \quad (29)$$

$$F_{\ell_j \rightarrow \ell_\alpha \gamma}(m_1, m_2) = \frac{2m_1^4 - 4m_1^2 m_2^2 + m_2^4 + 4m_1^4 \ln \left[\frac{m_2}{m_1} \right]}{2(m_1^2 - m_2^2)^3}. \quad (30)$$

Through the same diagram for the above LFVs, with $j = \alpha = 2$, there exists the contribution to $(g - 2)_\mu$ denoted by Δa_μ which is simply given by

$$\Delta a_\mu \approx -\frac{m_\mu a_{22}}{2}. \quad (31)$$

This value can be tested by current and future experiments [9, 10, 11].

Secondly we consider the $\mu - e$ conversion process which can be found in the same diagram as the process of $\ell_j \rightarrow \ell_\alpha \gamma$ with γ line being attached to nucleons and additional contribution is taken into account by replacing γ with Z boson. Then the $\mu - e$ conversion rate R is obtained as [12]

$$R \equiv \frac{\Gamma(\mu \rightarrow e)}{\Gamma_{\text{capt}}} = \frac{C_{\mu e}}{\Gamma_{\text{capt}}} \left| Z \left(b_{21}^\gamma - \frac{a_{21}}{m_\mu} \right) - b_{21}^Z \frac{(2Z + N)A_u + (Z + 2N)A_d}{2(s_{tw}c_{tw})^2} \right|^2, \quad (32)$$

$$b_{21}^V = \frac{s_{RCR}}{2\sqrt{2}(4\pi)^2} \sum_{k=1}^2 (y'_\ell)_{\alpha k} m_{L'_k} (y_{L'})_{k,j} \left[F_{\mu e}(m_{H_1}, m_{L'_k}, m_V) - F_{\mu e}(m_{H_2}, m_{L'_k}, m_V) \right], \quad (33)$$

$$F_{\mu e}(m_1, m_2, m_3) = \int_0^1 dx_3 \int_0^{1-x_3} dx_4 \frac{x_4(1-x_4)}{x_3 m_1^2 + (1-x_3)m_2^2 + x_4(x_3 + x_4 - 1)m_3^2}, \quad (34)$$

where $C_{\mu e} \equiv 4\alpha_{\text{em}}^5 \frac{Z_{\text{eff}}^4 |F(q)|^2 m_\mu^5}{Z}$, $A_u \equiv -\frac{1}{2} - \frac{4}{3}s_{tw}^2$, $A_d \equiv -\frac{1}{2} + \frac{2}{3}s_{tw}^2$, $\sin^2 \theta_w \equiv s_{tw}^2 \approx 0.23$, $V \equiv (\gamma, Z)$, $m_\gamma = 0$, and $m_Z \approx 91.19$ GeV. The values of Γ_{capt} , Z , N , Z_{eff} , and $F(q)$ depend on the type of nuclei. Here we consider Titanium case, because its sensitivity will be improved by several orders of magnitude [8] in near future compared to the current bound [7], as can be seen in the Table 3. In this case, we apply $\Gamma_{\text{capt}} = 2.59 \times 10^6 \text{ sec}^{-1}$, $Z = 22$, $N = 26$, $Z_{\text{eff}} = 17.6$, and $|F(-m_\mu^2)| = 0.54$ [13].

2.4. Numerical analysis

Now that we have all the formulae for the quark and lepton sector, we carry out numerical analysis to search for the preferred parameter range. Then we randomly select values of the fifteen parameters within the corresponding ranges

$$m_{\eta_I} \in [250 \text{ GeV}, 500 \text{ GeV}], \quad m_{H_1} \in [600 \text{ GeV}, 800 \text{ GeV}], \quad m_{H_2} \in [4 \text{ TeV}, 6 \text{ TeV}], \quad (35)$$

$$m_{Q'_1} \in [4.5 \text{ TeV}, 5 \text{ TeV}], \quad m_{Q'_2} \in [1.7 \text{ TeV}, 2.2 \text{ TeV}],$$

$$m_{L'_1} \in [7 \text{ TeV}, 7.5 \text{ TeV}], \quad m_{L'_2} \in [9 \text{ TeV}, 10 \text{ TeV}], \quad (36)$$

$$\{(y_u)_{12}, (y_u)_{22}\} \in [-1, 1], \quad (y_u)_{11} \in [-0.1, 0.1], \quad (y_u)_{21} \in [-0.002, 0.002],$$

$$\{(y_\nu)_{21}, (y_\nu)_{22}\} \in [-7 \times 10^{-12}, 7 \times 10^{-12}], \quad (y_\nu)_{11} \in [-3 \times 10^{-13}, 3 \times 10^{-13}],$$

$$(y_\nu)_{12} \in [-2 \times 10^{-13}, 2 \times 10^{-12}], \quad (37)$$

to reproduce quark and charged lepton masses, CKM matrix, and to fit neutrino oscillation data while satisfying the constraints of LFVs and FCNC. Note that the other Yukawa couplings such as y_Q , y_d , y_L , y_ℓ are numerically solved by using the best fit values of the measurements for quark [14] and lepton sector [15]. Generating randomly 10^7 sample points, we obtain 734 allowed points where the most stringent constraint comes from the process of $\mu \rightarrow e\gamma$. We also show some indication of the model in Fig. 2; the left figure is the scattering plot for Δm_D and Δm_K normalized by $[\text{MeV}] \times 10^{12}$, and the black solid lines represents the experimental upper bound while the right figure is the scattering plot for $\Delta a_\mu \times 10^{12}$ and $R_{Ti} \times 10^{17}$. Our Δm_K values are the same order as our phenomenological constraint and some parameter sets are excluded, and Δm_D values can be comparable to the constraint, which can be tested in the near future.

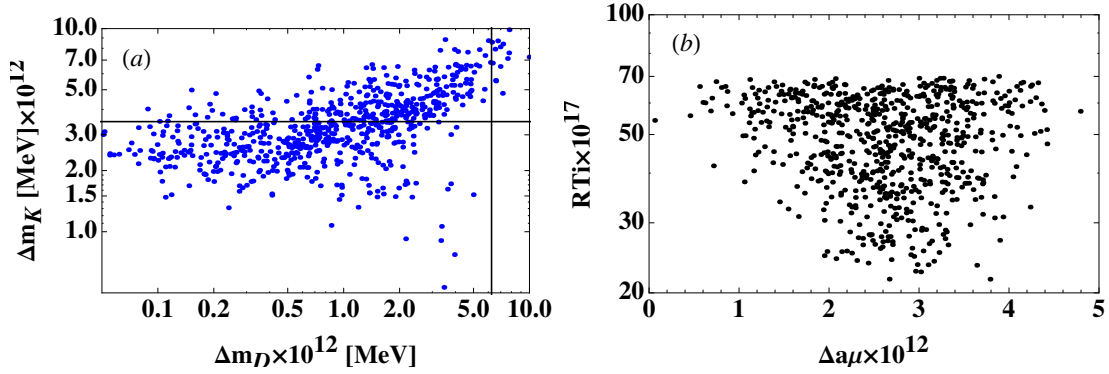


Figure 2. (a): The scattering plot in terms of Δm_D and Δm_K normalized by $[\text{MeV}] \times 10^{12}$, and the black solid lines represents the observed values. (b): The scattering plot in terms of $\Delta a_\mu \times 10^{12}$ and $R_{Ti} \times 10^{17}$.

Table 4. The charge assignments of lepton and scalar field sector in model II.

Fieldes	L_L^α	e_R^i	τ_R	$L_{L,R}^i$	N_R^i	N_L^i	Φ	φ	η	Φ_2	S	S^-
$SU(2)_L$	2	1	1	2	1	1	2	1	2	2	1	1
$U(1)_Y$	$-\frac{1}{2}$	-1	-1	$-\frac{1}{2}$	0	0	$\frac{1}{2}$	0	$\frac{1}{2}$	$\frac{1}{2}$	0	-1
$U(1)_R$	0	$-x$	0	0	x	0	0	x	x	$-x$	0	0
Z_2	$+$	$+$	$+$	$-$	$-$	$-$	$+$	$+$	$-$	$+$	$-$	$+$

We also find that the maximal value for $(g-2)_\mu$ is around 5×10^{-12} , which is lower than the current bound by three order of magnitude, and that R_{Ti} is also much lower than the current bound, however, it will be tested in the future experiment such as COMET [8], which will reach $R \approx 10^{-18}$.

3. Model II

In this section, we extend the model in previous section and discuss neutrino mass matrix which is generated at two-loop level [2].

3.1. Structure of the model

The structure of the model is similar to that in previous section where the applied symmetry is the same. The lepton sector and scalar filed sectors are extended as in the Table. 4; we assigned Z_2 odd parity to right-handed neutrino to forbid neutrino mass at tree and one-loop level, and introduced new gauge singlet fermion N_L , Higgs doublet with $U(1)_R$ charge Φ_2 and charged singlet scalar S^- . Note that we do not have Dirac mass term of SM neutrino due to Z_2 parity while $N_{R,L}$ has Dirac mass via VEV of φ . In our extension, we have two physical charged scalar components and the mass eigensates are given by

$$\begin{bmatrix} S^\pm \\ \phi_2^\pm \end{bmatrix} \equiv \begin{bmatrix} \cos C & \sin C \\ -\sin C & \cos C \end{bmatrix} \begin{bmatrix} H_1^\pm \\ H_2^\pm \end{bmatrix}. \quad (38)$$

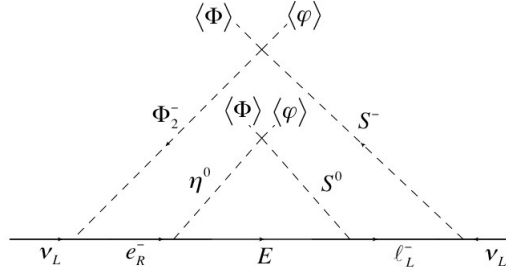


Figure 3. The two loop diagram for generating Majorana mass term for active neutrinos.

The new terms in Lagrangian of the model II are

$$-\mathcal{L} \supset (y'_\ell)_{\alpha j} \bar{L}_\alpha \Phi_2 e_{Rj} + (y'_S)_{\alpha\beta} \bar{L}_\alpha^C (i\sigma_2) L_\beta S^+ - \lambda_1 [\Phi^T (i\sigma_2) \Phi_2] \varphi S^- + \text{c.c.}, \quad (39)$$

and Yukawa interactions with y_ν coupling in Eq. (2) are now forbidden by Z_2 symmetry.

3.2. Neutrino mass matrix

As a consequence of the extending the model, the dominant contribution to the active neutrino mass matrix m_ν is now given at two-loop level where the corresponding diagram is shown in Fig. 3. Calculating the diagram, we then obtain the analytic form of neutrino mass matrix:

$$(m_\nu)_{ab} = -s_R c_R s_C c_C \frac{(y_\ell)_{ai} (y'_\ell)_{ij} \mathcal{M}_{E_j} (y'_S)_{jk} (y'_S)_{kb} + [(y_\ell)_{ai} (y'_\ell)_{ij} \mathcal{M}_{E_j} (y'_S)_{jk} (y'_S)_{kb}]^T}{2(4\pi)^4}, \quad (40)$$

$$\begin{aligned} \mathcal{M}_{E_j} &\equiv m_{L'_j} \int [dx] \int [dX] \frac{y}{(x_4 - 1)^2} \ln \left(\frac{\Delta_3[E_j, H_1^\pm, H_2] \Delta_3[E_j, H_2^\pm, H_1]}{\Delta_3[E_j, H_1^\pm, H_1] \Delta_3[E_j, H_2^\pm, H_2]} \right), \\ \Delta_3[a, b, c] &\equiv x m_a^2 - \frac{y(x_3 m_b^2 + x_4 m_c^2)}{x_4^2 - x_4}, \quad \int [dx] \equiv \int_0^1 dx \int_0^{1-x} dy \delta(1 - x - y), \\ \int [dX] &\equiv \int_0^1 dx_1 \int_0^{1-x_1} dx_2 \int_0^{1-x_1-x_2} dx_3 \int_0^{1-x_1-x_2-x_3} dx_4 \delta(1 - x_1 - x_2 - x_3 - x_4). \end{aligned} \quad (41)$$

The neutrino mass matrix $(m_\nu)_{ab}$ can generally be diagonalized by use of the mixing matrix V_{MNS} (PMNS) and can be written in terms of experimental values depending on the normal hierarchy (NH) and inverted hierarchy (IH) as follows:

$$(m_\nu)_{ab}^{\text{exp.}} = (V_{\text{MNS}} D_\nu V_{\text{MNS}}^T)_{ab}, \quad D_\nu \equiv (m_{\nu_1}, m_{\nu_2}, m_{\nu_3})$$

$$\text{(NH)} : |m_\nu^{\text{exp.}}| \approx \begin{bmatrix} 0.0845 - 0.475 & 0.0629 - 0.971 & 0.0411 - 0.964 \\ * & 1.44 - 3.49 & 1.94 - 2.85 \\ * & * & 1.22 - 3.33 \end{bmatrix} \times 10^{-11} \text{ GeV}, \quad (42)$$

$$\text{(IH)} : |m_\nu^{\text{exp.}}| \approx \begin{bmatrix} 0.993 - 4.96 & 0.00261 - 3.83 & 0.00280 - 3.95 \\ * & 0.00380 - 3.08 & 0.345 - 2.61 \\ * & * & 0.000647 - 3.30 \end{bmatrix} \times 10^{-11} \text{ GeV}, \quad (43)$$

$$V_{\text{MNS}} = \begin{bmatrix} c_{13}c_{12} & c_{13}s_{12} & s_{13}e^{-i\delta} \\ -c_{23}s_{12} - s_{23}s_{13}c_{12}e^{i\delta} & c_{23}c_{12} - s_{23}s_{13}s_{12}e^{i\delta} & s_{23}c_{13} \\ s_{23}s_{12} - c_{23}s_{13}c_{12}e^{i\delta} & -s_{23}c_{12} - c_{23}s_{13}s_{12}e^{i\delta} & c_{23}c_{13} \end{bmatrix} \begin{bmatrix} e^{i\alpha_1/2} & 0 & 0 \\ 0 & e^{i\alpha_2/2} & 0 \\ 0 & 0 & 1 \end{bmatrix}, \quad (44)$$

where we have used the following neutrino oscillation data at 3σ [15]:

$$\text{(NH)} : 0.278 \leq s_{12}^2 \leq 0.375, 0.392 \leq s_{23}^2 \leq 0.643, 0.0177 \leq s_{13}^2 \leq 0.0294, \delta \in [-\pi, \pi],$$

$$m_{\nu_3} = (\sqrt{23.0} - \sqrt{26.5}) \times 10^{-11} \text{ GeV}, \quad m_{\nu_2} = (\sqrt{0.711} - \sqrt{0.818}) \times 10^{-11} \text{ GeV}, \quad (45)$$

$$\text{(IH)} : 0.278 \leq s_{12}^2 \leq 0.375, 0.403 \leq s_{23}^2 \leq 0.640, 0.0183 \leq s_{13}^2 \leq 0.0297, \delta \in [-\pi, \pi],$$

$$m_{\nu_1} = (\sqrt{22} - \sqrt{25.4}) \times 10^{-11} \text{ GeV}, \quad m_{\nu_2} = (\sqrt{22.711} - \sqrt{26.218}) \times 10^{-11} \text{ GeV}, \quad (46)$$

and the two Majorana phases $\alpha_{1,2}$ are taken to be $\alpha_{1,2} \in [-\pi, \pi]$ in both cases. Notice that we assume one of three neutrino masses is zero, which is predicted by the theoretical aspect that y'_S is anti-symmetric matrix, i.e. the rank of neutrino mass matrix is reduced to two. Applying the above properties, we can rewrite two components of y'_S by experimental values and one of the component of y'_S as follows ¹:

$$\text{(NH)} : (y'_S)_{e\tau} = \left(\frac{s_{12}c_{23}}{c_{12}c_{13}} + \frac{s_{13}s_{23}}{c_{13}} e^{-i\delta} \right) (y'_S)_{\mu\tau}, \quad (y'_S)_{e\mu} = \left(\frac{s_{12}c_{23}}{c_{12}c_{13}} - \frac{s_{13}s_{23}}{c_{13}} e^{-i\delta} \right) (y'_S)_{\mu\tau}, \quad (47)$$

$$\text{(IH)} : (y'_S)_{e\tau} = -\frac{s_{23}}{t_{13}} (y'_S)_{\mu\tau}, \quad (y'_S)_{e\mu} = \frac{c_{23}}{t_{13}} (y'_S)_{\mu\tau}, \quad (48)$$

where the explicit form of y'_S is given as

$$(y'_S) \equiv \begin{bmatrix} 0 & (y'_S)_{e\mu} & (y'_S)_{e\tau} \\ -(y'_S)_{e\mu} & 0 & (y'_S)_{\mu\mu} \\ -(y'_S)_{e\tau} & -(y'_S)_{\mu\tau} & 0 \end{bmatrix}. \quad (49)$$

In our numerical analysis, only $(y'_S)_{\mu\tau}$ is an input parameter, and we will search for the allowed parameter region by comparing the experimental values in Eqs. (42) and (43).

3.3. Numerical analysis

Finally, we carry out numerical analysis to search for the parameter region that can fit the experimental data. To reduce the number of free parameters, we first fix some parameters such that; $s_\beta = 0.3$, $s_R = 0.1$, $s_C = 1$, $m_{h_1} = 4 \text{ TeV}$. Then we randomly select values of masses as $M_X \equiv m_{H_1} \in [0, 10] \text{ TeV}$, $m_{H_2^\pm} \in [11M_X/10, 12M_X/10] \text{ TeV}$, $m_{L'_1} \in [11M_X/10, 9] \text{ TeV}$, $m_{L'_2} \in [m_{L'_1}, 9.5] \text{ TeV}$, $m_{L'_3} \in [m_{L'_2}, 10] \text{ TeV}$, and $m_{\eta^\pm} = m_{H_2} \in [11M_X/10, 12(11.1)M_X/10]$. Then, we randomly select values of the dimensionless parameters within $[-1, 1]$ to search for allowed parameter region. As a result we find the allowed ranges for our Yukawa couplings in both NH and IH cases:

$$(y'_S)_{\mu\tau} \in [-0.027, 0.027], \quad (50)$$

$$y_L = \begin{bmatrix} 0.01 - 0.135 & -(0.025 - 0.02) & -(0.0265 - 0.02) \\ 0.03 - 0.036 & 0.01 - 0.015 & -(0.045 - 0.04) \\ -(0.027 - 0.02) & -(0.0208 - 0.02) & -(0.028 - 0.02) \end{bmatrix},$$

$$y'_\ell = \begin{bmatrix} -(0.016 - 0.01) & 0.04 - 0.0453 & -(0.02 - 0.01) \\ -(0.0063 - 0.001) & 0.04 - 0.05 & -(0.031 - 0.01) \\ 0.001 - 0.0012 & -(0.0174 - 0.01) & 0.03 - 0.036 \end{bmatrix},$$

$$y_\ell = \begin{bmatrix} 0.03 - 0.037 & -(0.0445 - 0.04) & 0.001 - 0.0088 \\ 0.01 - 0.0123 & 0.02 - 0.0275 & -(0.032 - 0.01) \\ 0.01 - 0.03 & 0.001 - 0.0094 & 0.001 - 0.005 \end{bmatrix}, \quad (51)$$

¹ The detailed analysis for both hierarchies can be found in Ref. [16].

which can reproduce neutrino oscillation data and satisfies the constraints from LFVs. Therefore we find that the hierarchy in the Yukawa couplings becomes smaller compared to the SM case. Note that the allowed parameter region can accommodate observed relic density of DM assuming H_1 to be our DM where detailed discussion can be found in Ref. [2].

4. Summary and discussion

We have reviewed two models in which light fermion masses are generated at loop levels. The Yukawa couplings with SM Higgs are restricted by introducing extra U(1) gauge symmetry and discrete Z_2 symmetry. Then first and second generation charged-lepton and quark masses are generated at one-loop level by introducing vector-like fermions and exotic scalars. In the first model, the SM neutrino masses are generated at one-loop level as the same way as other fermion sectors, which require tiny Yukawa coupling constants. On the other hand, the neutrino masses are generated at two-loop level in the second model which is the extension of first one.

We presented the formulas for fermion mass matrices, lepton flavor violations and flavor changing neutral current effect on meson anti-meson ($Q-\bar{Q}$) mixing. Then numerical calculation is carried out to search for the parameter range to fit the observed data. We find that our Yukawa couplings can be less hierarchical compared to SM case due to loop induced mass for first two generations. In particular, in the second model, we can generate tiny neutrino mass with $\mathcal{O}(10^{-3})$ to $\mathcal{O}(1)$ Yukawa coupling constants through two-loop level effect. We also show some implication of the model in $\mu-e$ conversion and $Q-\bar{Q}$ mixing which can be tested in future experiment. In addition, collider physics of our exotic particles will be interesting and it is left as future works.

References

- [1] Nomura T, Okada H 2016 *Phys. Lett. B* **761** 190
- [2] Nomura T, Okada H 2016 *Phys. Rev. D* **94** no. 9 093006
- [3] Gabbiani F, Gabrielli E, Masiero A, Silvestrini L 1996 *Nucl. Phys. B* **477** 321
- [4] Okada H, Okada N, Orikasa Y, Yagyu K 2016 *Phys. Rev. D* **94** no. 1 015002
- [5] Baldini A M *et al.* [MEG Collaboration] 2016 *Eur. Phys. J. C* **76** no. 8 434
- [6] Adam J, *et al.* [MEG Collaboration] 2013 *Phys. Rev. Lett.* **110** 201801
- [7] Dohmen C, *et al.* [SINDRUM II Collaboration] 1993 *Phys. Lett. B* **317** 631
- [8] Hungerford E V [COMET Collaboration] 2009 *AIP Conf. Proc.* **1182** 694
- [9] Bennett G W, *et al.* [Muon G-2 Collaboration] 2006 *Phys. Rev. D* **73** 072003
- [10] Jegerlehner F, Nyffeler A 2009 *Phys. Rept.* **477** 1
- [11] Benayoun M, David P, Delbuono L, Jegerlehner F 2012 *Eur. Phys. J. C* **72** 1848
- [12] Hisano J, Moroi T, Tobe K, Yamaguchi M 1996 *Phys. Rev. D* **53** 2442
- [13] Alonso R, Dhen M, Gavela M B, Hambye T 2013 *JHEP* **1301** 118
- [14] Olive K A, *et al.* (Particle Data Group) 2014 *Chin. Phys. C* **38** 090001
- [15] Forero D V, Tortola M, Valle J W F 2014 *Phys. Rev. D* **90** no. 9 093006
- [16] Herrero-Garcia J, Nebot M, Rius N, Santamaria A 2014 *Nucl. Phys. B* **885** 542